Advances in Concrete Construction, *Vol. 2, No. 3 (2014) 229-247*
DOI: http://dx.doi.org/10.12989/acc.2014.2.3.229

Effect of shear-span/depth ratio on cohesive crack and double-*K* fracture parameters of concrete

Rajendra Kumar Choubey[a] and Shailendra Kumar[*] and M.C. Rao[b]

Department of Civil Engineering, Institute of Technology, Guru Ghasidas Vishwavidyalaya (A Central University), Bilaspur (C.G.) - 495009, India

(Received January 1, 2014, Revised November 6, 2014, Accepted November 7, 2014)

Abstract. A numerical study of the influence of shear-span/depth ratio on the cohesive crack fracture parameters and double – *K* fracture parameters of concrete is carried out in this paper. For the study the standard bending specimen geometry loaded with four point bending test is used. For four point loading, the shear – span/depth ratio is varied as 0.4, 1 and 1.75 and the ao/D ratio is varied from 0.2, 0.3 and 0.4 for laboratory specimens having size range from 100 – 500 mm. The input parameters for determining the double – *K* fracture parameters are taken from the developed fictitious crack model. It is found that the cohesive crack fracture parameters are independent of shear-span/depth ratio. Further, the unstable fracture toughness of double-*K* fracture model is independent of shear-span/depth ratio whereas, the initial cracking toughness of the material is dependent on the shear-span/depth ratio.

Keywords: four-point bend test; shear-span depth ratio; cohesive crack fracture parameters; double-*K* fracture parameters; weight function; cohesive stress

1. Introduction

The principle of linear elastic fracture mechanics (LEFM) was first applied by Kaplan (1961) to notched concrete beam for determining the critical stress intensity factor of concrete. Thereafter, until early 1970s numerous experimental and numerical investigations using linear elastic fracture mechanics were carried out to study the fracture process and crack propagation of concrete. From the studies, it was understood that LEFM could be only applied to large-mass concrete structures and could not be applied to medium and small-scale concrete structures. The inapplicability of LEFM is attributed mainly to the nonlinear effects associated with crack propagation in concrete. It is well understood that before the development of unstable crack, due to the aggregate interlocking property, there exists a large fracture process zone ahead of initial crack tip, which is primarily responsible for the size effect behavior. Since late 1970s, many nonlinear fracture models incorporating the tension softening property of the material have been developed by various groups of researchers to study the behavior of crack propagation in *quasibrittle* materials

∗Corresponding author, E-mail: Professor, E-mail: shailendrakmr@yahoo.co.in
[a]Ph.D. Student and Assistant Professor
[b]Associate Professor

http://www.techno-press.org/?journal=acc&subpage=7 ISSN:2287-5301(Print)2287-531X(Online)

like concrete. The nonlinear fracture models applied to concrete structures are: cohesive crack model (CCM) or fictitious crack model (FCM) (Hillerborg *et al*. 1976), crack band model (CBM) (Bažant and Oh 1983), two parameter fracture model (TPFM) (Jenq and Shah 1985a), size effect model (SEM) (Bažant *et al*. 1986), effective crack model (ECM) (Nallathambi and Karihaloo 1986), K_R-curve method based on cohesive force distribution (Xu and Reinhardt 1998, 1999a), double-*K* fracture model (DKFM) (Xu and Reinhardt 1999a-c) and double-*G* fracture model (DGFM) (Xu and Zhang 2008).

The cohesive crack model, based on numerical approach is a simplified nonlinear fracture model which can simulate satisfactorily the complex nonlinear phenomena in the fracture process zone of concrete and it predicts the localized real physical behavior in the vicinity of a crack and at the crack tip. Based on early stage of development of the fracture models (Barenblatt 1959, Dugdale 1960), Hillerborg and co-workers (Hillerborg *et al*. 1976) initially applied cohesive crack method (or fictitious crack model) as a suitable nonlinear model for mode I fracture to simulate the softening damage of concrete structures. The authors showed that analysis of crack formation, crack propagation and failure analysis can be done with cohesive crack model even if coarse finite element is used thereby eliminating the mesh sensitivity. A brief overview of the cohesive crack model, its numerical aspects, advantages, limitations and challenges can be seen elsewhere (Guinea 1995, Elices and Planas 1996, Bažant 2002, Elices *et al*. 2002, de Borst 2003, Planas *et al*. 2003, Carpinteri *et al*. 2003, Carpinteri *et al*. 2006). Numerous experimental and numerical studies based on cohesive crack model have been carried out many researchers (Petersson 1981, Carpinteri 1989, Planas and Elices 1991, Zi and Bažant 2003, Kim *et al*. 2004, Roesler *et al*. 2007, Raghu Prasad and Renuka Devi 2007, Park *et al*. 2008, Zhao *et al*. 2008, Kwon *et al*. 2008, Cusatis and Schaffert 2009, Elices *et al*. 2009, Kumar and Barai 2008b-2009c). The authors (Kumar and Barai, 2008b, 2009c) presented numerical study on the fracture parameters of concrete using three point bend test (Kumar and Barai 2008b) and compact tension test (Kumar and Barai 2009c) specimens of different sizes using cohesive crack model. In the study (Kumar and Barai 2008b) it was observed that the values of peak load for three point bend test determined using numerical results were not greatly affected by refinement of finite element mesh however, the values of the peak load is influenced by choice of softening functions. Kumar and Barai (2009c) presented that the result of peak loads, the fracture process zones, crack-tip opening displacement at peak load and value of the tip stress transfer ratio at peak load obtained using compact tension test is influenced by specimen size and softening functions.

The past experimental results show that the fracture process of concrete structures includes three main stages: (i) crack initiation, (ii) stable crack propagation, and (iii) unstable fracture and the double-K fracture model based on modified LEFM can describe the above three important stages of crack propagation in concrete without much difficulty in conducting the experiment as well as in computation of the fracture parameters. This method does not require closed loop testing system in the laboratory. The double-K fracture model is characterized by two material parameters: initial cracking toughness K_{IC}^{ini} and unstable fracture toughness K_{IC}^{un}. The initiation toughness is defined as the inherent toughness of the materials, which holds for loading at crack initiation when material behaves elastically and micro cracking is concentrated to a small-scale in the absence of main crack growth. It is directly calculated by knowing the initial cracking load and initial notch length using LEFM formula. The total toughness at the critical condition is known as unstable toughness K_{IC}^{un} which is regarded as one of the material fracture parameters at the onset of the unstable crack propagation. This parameter can be obtained by knowing peak load and corresponding effective crack length using the same LEFM formula. In the past, extensive

numerical and experimental studies (Xu and Reinhardt 1999a-c, Xu and Reinhardt 2000, Zhao and Xu 2002, Zhang *et al*. 2007, Xu and Zhu 2009, Kumar and Barai 2008a, 2009a-b, 2010a-b, 2012, Zhang and Xu 2011, Kumar and Pandey 2012, Hu and Lu 2012, Murthy *et al*. 2012, Hu *et al*. 2012, Yu and Lu 2013, Kumar *et al*. 2013) have been carried out for the study on fracture parameters of concrete using double – *K* model with different tests specimens. With respect to numerical studies in recent time, Zhao and Xu (2002) put forward numerical investigation of the effect of span/ depth ratio ranging from 3 to 8 with three point bend specimen on the double – *K* fracture parameters. The numerical investigation showed that the unstable fracture toughness is independent of span/ depth ratio and depends only on the material property. While the initiation fracture toughness not only varies with the strength of material, but also presents size effects in terms of span/ depth ratio and the depth of specimens. The authors (Kumar and Barai 2008a, 2009b, 2012) showed that the double-*K* fracture parameters are influenced by the specimen geometry, size-effect, relative size of initial crack length and softening function of concrete. It was further reported that the double-*K* fracture parameters marginally depend on the loading condition. Prediction of size-effect from double-*K* fracture parameters was also formulized in a study by Kumar and Barai (2010b).

In continuation of previous studies, this paper presents a numerical study of the influence of shear-span/depth ratio on the cohesive crack fracture parameters and double – *K* fracture parameters of concrete using the standard bending specimen geometry loaded with four point bending test. For four point loading, the shear – span/depth ratio is varied from 0.4D, D and 1.75D and the a_o/D ratio is varied from 0.2 to 0.4 for laboratory size specimen ranging from 100 mm to 500 mm. To this end, a brief introduction of double – *K* fracture model and cohesive crack model is presented in the subsequent sections.

2. Specimen geometry

The standard notched beam specimen used for three-point bend test (TPBT) (RILEM Technical Committee 50-FMC 1985) with four-point loading is considered in the present study. Like three-point bending test, the fracture parameters of the four-point bending test can be easily determined. The dimensions of the four point bending test (FPBT) geometry are shown in Fig.1 in which, the symbols: *B*, *D*, *S* and L are the width, depth, support span and moment arm or shear – span respectively with *S/D* = 4. The shear – span/depth (L/D) ratio is varied as 0.4, 1 and 1.75 in the present work.

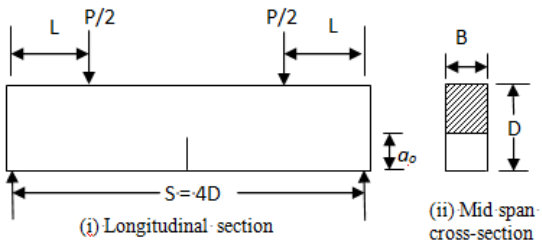

Fig. 1 Dimensions and loading schemes of four-point bending test specimen

3. Determination of double-*K* fracture parameters

The double-*K* fracture parameters can be determined using experimental test results in which the primary requirement is to measure the initial cracking load P_{ini}, initial crack length a_o, peak load P_u and crack mouth opening displacement at peak load $CMOD_c$ from the tests. In order to apply LEFM equations for calculating the double-K fracture parameters, Xu and Reinhardt (1999b) introduced linear asymptotic superposition assumption. The hypotheses of the assumption are given below:

1. the nonlinear characteristic of the load-crack mouth opening displacement (P-CMOD) curve is caused by fictitious crack extension in front of a stress-free crack, and
2. an effective crack consists of an equivalent-elastic stress-free crack and equivalent-elastic fictitious crack extension.

A detailed explanation of the hypotheses may be seen elsewhere (Xu and Reinhardt 1999b).

3.1 Effective crack extension

The values of P_u and $CMOD_c$ from the four-point bend tests are obtained and then applying linear asymptotic superposition assumption the equivalent-elastic crack length a_c at maximum load is be solved using LEFM formulae. For the pure bending case (four-point bending test with S/D=4), the following formulae (Tada *et al*. 2000) are used to calculate the equivalent crack extension.

$$CMOD = \frac{12PLa}{BD^2E}V_1(\beta) \tag{1}$$

$$V_1(\beta) = 0.8 - 1.7\beta + 2.4\beta^2 + \frac{0.66}{(1-\beta)^2} \tag{2}$$

where, $\beta = (a+H_o)/(D+H_o)$ and H_o = thickness of the clip gauge holder. Eq. (2) has better than 1% accuracy for any value of β. Similarly, the measured initial compliance C_i from the P-CMOD curve can be used to calculate the E as per the following formula.

$$E = \frac{12La_o}{C_iBD^2}V_1(\beta_o) \tag{3}$$

where, $\beta_o = (a_o+H_o)/(D+H_o)$ and a_o = initial crack length. For the precise numerical investigation, the effect of self-weight in four-point bending test geometries can be accounted for at all computation stages. Hence, in addition to the external load *P/2* acting on the four-point bending test, the influence due to a concentrated load equal to $w_g.S/2$ and acting at the mid span, is also effective during all stages of the computations. The contribution of the concentrated load ($w_g.S/2$) acting at mid span due to self weight of the beam in the crack mouth opening displacement (CMOD) due to TPBT action is taken into account while calculating the equivalent effective crack extension in case of four-point bending test specimen. For TPBT with S/D = 4 using LEFM formulae (Tada *et al*. 2000) the value of CMOD can be expressed as

$$CMOD = \frac{6\left(w_g S/2\right)Sa}{BD^2E}V_2(\beta) \tag{4}$$

$$V_2(\beta) = 0.76 - 2.28\beta + 3.87\beta^2 - 2.04\beta^3 + \frac{0.66}{(1-\beta)^2} \tag{5}$$

The measured initial compliance C_i from the P-CMOD curve is used to calculate the Young's modulus E as per the RILEM (1990) formula.

$$E = \frac{6Sa_o}{C_i BD^2}V_2(\beta_o) \tag{6}$$

Finally, considering the effect of self weight of the beam, the total CMOD for the four-point bending test specimen can be written as:

$$CMOD = \frac{3a}{BD^2E}\left[4PLV_1(\beta) + w_g S^2 V_2(\beta)\right] \tag{7}$$

Eq.(7) accounts for the self weight for beam while calculating the CMOD for pure bending case specimen. At unstable fracture i.e., at peak load the values of $CMOD = CMOD_c$ and $a = a_c$. It was concluded (Karihaloo and Nallathambi 1991) that almost the same value of E might be obtained from P-CMOD curve, load-deflection curve and compressive cylinder test. Hence, in case initial compliance is not known the value of E determined using compressive cylinder tests may be used to obtain the critical crack length of the specimen.

3.2 Computation of double-K fracture parameters

The cohesive stress distribution in the fictitious crack zone which gives rise to cohesion toughness as a part of total toughness of the cracked body. Superposition method is used in order to calculate the stress intensity factor at the tip of effective crack length K_I. According to this scheme, total stress intensity factor K_I is equal to the summation of stress intensity factor caused due to external load K_I^P and the stress intensity factor contributed by cohesive stress K_I^C (Jenq and Shah 1985b, Xu and Reinhardt 1999b) as shown in Fig. 2. The value of K_I is expressed in the following expression:

$$K_I = K_I^P + K_I^C \tag{8}$$

After determining the critical effective crack extension at unstable condition of loading, the two parameters (K_{IC}^{ini} and K_{IC}^{un}) of double-*K* fracture model is determined using LEFM formulae. The total stress intensity factor at the tip of fictitious crack in case of pure bending specimen can be determined due to the load on the beam which consists of two parts, the first is the external load and the second is the self weight of the beam. The external load is considered to act on four point bend test specimen where as the effective load equal to $w_g S/2$ is considered to be acting on standard three point bend test specimen. This yields precise determination of the stress intensity factor accounting for the self weight of the specimen. The stress intensity factor for the four-point bending test, K_I due to external load and self-weight of the beam at any loading stage can be calculated using the following procedures. The stress intensity factor due to external load p on the four-point bending test specimen K_I^E (Murakami 1987) is expressed as:

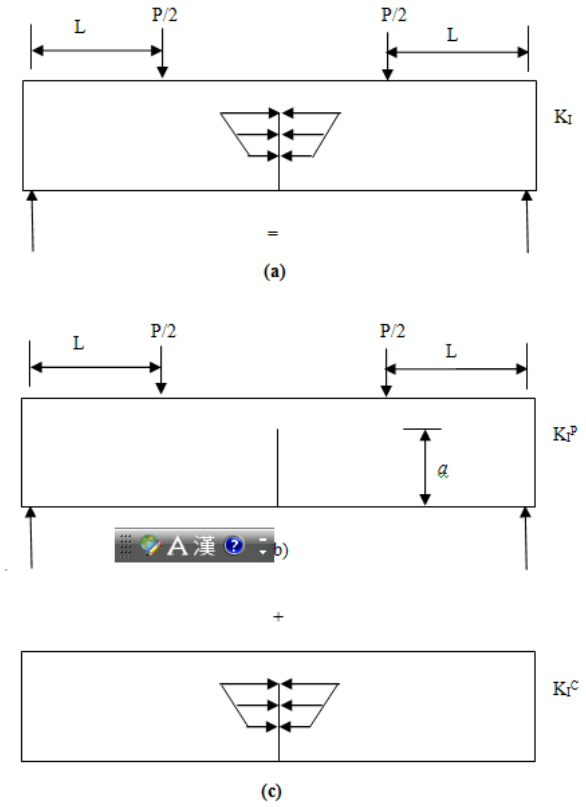

Fig. 2 Calculation of stress intensity factor using superposition method

$$K_I^{\ E} = \sigma_{NE}\sqrt{D}F_{IP}k_1(\alpha) \tag{9}$$

$$\sigma_{NE} = \frac{3PL}{BD^2} \tag{10}$$

$$k_1(\alpha) = \sqrt{\pi\alpha}\left\{1.122 - 1.121\alpha + 3.740\alpha^2 + 3.873\alpha^3 - 19.05\alpha^4 + 22.55\alpha^5\right\} \tag{11}$$

where, F_{IP} in Eq.(9) is a coefficient which accounts for the difference between four point bending and pure bending cases. The value of F_{IP} for shear-span depth ratios of 0.4 and 1 converges to 1 (Murakami 1987). In the present study, the value of F_{IP} is taken as unity for shear-span depth ratios of 0.4 and 1, whereas, it is read from the graph given in Murakami (1987) for shear-span depth ratio 1.75. Eq. (11) has better than 1% accuracy for $\alpha \leq 0.7$. The contribution of stress intensity factor due to self weight of the specimen K_I^S (considering TPBT for S/D = 4) is expressed as **(**Tada *et al*. 2000**)**:

$$K_I^{\ S} = \sigma_{NS}\sqrt{D}k_2(\alpha) \tag{12}$$

$$\sigma_{NS} = \frac{3w_g S^2}{4bD^2} \tag{13}$$

$$k_2(\alpha) = \sqrt{\alpha}\,\frac{1.99 - \alpha(1-\alpha)(2.15 - 3.93\alpha + 2.7\alpha^2)}{(1+2\alpha)(1-\alpha)^{3/2}} \tag{14}$$

in which, α is *a/D*, $k_2(\alpha)$ is obtained using expression (14). The values of σ_{NE} and σ_{NS} are the nominal stresses in the beam due to external load *P* and self weight of the structure respectively. Hence effective stress intensity factor K_I of the four-point bending test loading condition can be obtained as the summation of the values K_I^E and K_I^S, which is given below:

$$K_I = \sqrt{D}\left[\sigma_{NE} F_{IP} k_1(\alpha) + \sigma_{NS} k_2(\alpha)\right] \tag{15}$$

The LEFM Eq. (15) can be used for calculation of unstable fracture toughness K_{IC}^{un} at the tip of effective crack length a_c, in which $a = a_c$ and P = maximum load P_u for four-point bending test specimen geometries. In case, when the crack initiation load from experimental is not available, an inverse analytical method is used to calculate the value of K_{IC}^{ini} which is given below.

$$K_{IC}^{ini} = K_{IC}^{un} - K_{IC}^{C} \tag{16}$$

where K_{IC}^{C} is the cohesive toughness of the material at peak load.

3.3 Determination of cohesive toughness

3.3.1 Cohesive stress distribution

The cohesive stress acting in the fictitious fracture zone in four-point bending test specimens is idealized as a series of pair normal forces subjected to single edge cracked specimen of finite width as shown in Fig. 3.

Fig. 4 presents the linearly varying distribution of cohesive stress in the fracture zone at peak load. The value of cohesion toughness K_{IC}^{C} is negative because of closing stress in fictitious crack zone. However, the absolute value of K_{IC}^{C} is taken as a contribution of the total fracture toughness. The same computation method (Jenq and Shah 1985b) of K_I^C has been also used in the analytical method (Xu and Reinhardt 1999b-c).

The σ_s ($CTOD_c$) denotes the value of cohesive stress at the tip of initial notch corresponding to crack tip opening displacement ($CTOD_c$) at peak load. Then the cohesive stress $\sigma(x)$ in fracture zone as shown in Fig.4 is expressed by following expression.

$$\sigma(x) = \sigma_s(CTOD_c) + \frac{x - a_o}{a - a_o}[f_t - \sigma_s(CTOD_c)] \; for \; 0 \le CTOD \le CTOD_c \tag{17}$$

The value of $\sigma_s(CTOD_c)$ is calculated by using softening functions of concrete such as bilinear, quasi-exponential, nonlinear, etc. However, in the present work, the nonlinear softening function (Reinhardt *et al*. 1986) is used for all computations which can be expressed as:

$$\sigma(w) = f_t \left\{ \left[1 + \left(\frac{c_1 w}{w_c} \right)^3 \right] \exp\left(\frac{-c_2 w}{w_c} \right) - \frac{w}{w_c}\left(1 + c_1^3\right)\exp\left(-c_2\right) \right\} \tag{18}$$

The value of total fracture energy of concrete G_F is written as:

$$G_F = w_c f_t \left\{ \frac{1}{c_2} \left[1 + 6\left(\frac{c_1}{c_2} \right)^3 \right] - \left[1 + c_1^3 \left(1 + \frac{3}{c_2} + \frac{6}{c_2^2} + \frac{6}{c_2^3} \right) \right] \frac{\exp\left(-c_2\right)}{c_2} - \left(\frac{1 + c_1^3}{2} \right) \exp\left(-c_2\right) \right\} \tag{19}$$

Where, $\sigma(w)$ is the cohesive stress at crack opening displacement w at the crack-tip and c_1 and c_2 are the material constants. w_c is the maximum crack opening displacement at the crack-tip at which the cohesive stress becomes to be zero. The value of w_c is determined using Eq. (19) for a given set of values c_1, c_2 and G_F. Since, it is difficult to measure directly the values of $CTOD_c$, for practical purposes the value of crack mouth opening displacement is measured. At critical condition, for the known value of $CMOD_c$ the crack opening displacement within the crack length $COD(x)$ is computed using the following expression (Jenq and Shah 1985a).

$$COD(x) = CMOD_c \left\{ (1 - x/a)^2 + (1.081 - 1.149a/D)[x/a - (x/a)^2] \right\}^{1/2} \tag{20}$$

In Eq. (20), the $COD(x)$ becomes $CTOD_c$ for given value of $x = a_o$ and $a = a_c$.

3.3.2 Computation of K_{IC}^C using weight function approach

The use of universal form of weight function method (Glinka and Shen 1991) was presented by Kumar and Barai (2008a, 2009a, 2010a) for determining the cohesive toughness of concrete. According to this method universal form of weight function having five terms for a single edge cracked specimen of finite width is expressed as

$$m(x,a) = \frac{2}{\sqrt{2\pi(a-x)}} \left[1 + M_1(1 - x/a)^{1/2} + M_2(1 - x/a) + M_3(1 - x/a)^{3/2} + M_4(1 - x/a)^2 \right] \tag{21}$$

In Eq.(21), first of all four parameters M_1, M_2, M_3 and M_4 of five-term universal weight function is determined in which the values of M_1, M_2 M_3 and M_4 can be represented as a function of a/D ratio in the following form.

$$M_i = \frac{1}{(1 - a/D)^{3/2}} \left[a_i + b_i a/D + c_i (a/D)^2 + d_i (a/D)^3 + e_i (a/D)^4 + f_i (a/D)^5 \right] \tag{22}$$

for, i = 1 and 3 and

$$M_i = \left[a_i + b_i a/D \right] \text{ for } i = 2 \text{ and } 4. \tag{23}$$

The values of coefficients a_i, b_i, c_i, . . ., f_i are given in Table 1.

Then the stress intensity factor using weight function method can be expressed as:

$$K = \int_0^a \sigma(x).m(x,a)dx \tag{24}$$

Table 1 Coefficients of five terms weight function parameters M_1, M_2, M_3 and M_4

i	a_i	b_i	c_i	d_i	e_i	f_i
1	-0.000824975	0.6878602	0.4942668	-3.25418434	3.4426983	-1.3689673
2	0.782308	-3.0488836				
3	-0.3049218	13.4186519	-23.31662697	35.51066606	-34.440981408	14.10339412
4	0.28347699	-7.378355423				

The value of $\sigma(x)$ in Eq. (24) is replaced by Eq. (17), hence a closed form expression for K_{IC}^{C} can be obtained as

$$K_{IC}^{C}=\frac{2}{\sqrt{2\pi a}}\left\{A_1 a\left[2s^{1/2}+M_1 s+\frac{2}{3}M_2 s^{3/2}+\frac{M_3}{2}s^2+\frac{2}{5}M_4 s^{5/2}\right]+\right.$$
$$\left.A_2 a^2\left[\frac{4}{3}s^{3/2}+\frac{M_1}{2}s^2+\frac{4}{15}M_2 s^{5/2}+\frac{4}{35}M_4 s^{7/2}+\frac{M_3}{6}\left\{1-(a_o/a)^3-3sa_o/a\right\}\right]\right\} \quad (25)$$

where, $A_1=\sigma_s(CTOD_c), A_2=\dfrac{f_t-\sigma_s(CTOD_c)}{a-a_o}$ and $s=(1-a_o/a)$. At the critical effective crack extension, a is equal to a_c in Eq. (25). After determining the value of K_{IC}^{C}, the value of K_{IC}^{ini} can be evaluated using Eq.(16).

4. Fictitious crack model

For development of cohesive crack model (CCM) or fictitious crack model (FCM) (Petersson 1981, Carpinteri 1989, Planas and Elices 1991, Zi and Bažant 2003, Kumar and Barai 2008b-2009c) three material parameters *i.e.*, modulus of elasticity E, uniaxial tensile strength f_t, and fracture energy G_F are required. The concrete mix with material properties: v = 0.18, f_t = 3.21MPa, E = 30 GPa, and G_F = 103N/m along with nonlinear stress-displacement softening relation with constants c_1 = 3 and c_2 = 7 are used as the input parameters in the present study. In this method, the governing equation of crack opening displacement (COD) along the potential fracture line is written. The influence coefficients of the COD equation are determined using linear elastic finite element method. Four noded isoparametric plane elements are used in finite element calculation. The COD vector is partitioned according to the enhanced algorithm introduced by Planas and Elices (1991). Finally, the system of nonlinear simultaneous equation is developed and solved using Newton-Raphson method. For pure bending test specimens with B = 100 mm having size range D = 100-500 mm, the finite element analysis is carried out for which the half of the specimens are discretized due to symmetry considering 80 numbers of equal isoparametric plane elements along the dimension D. The descritization of pure bending specimens at L = 0.4D, L= D and L = 1.75D is shown in Fig. 5.

Two more fracture parameters such as brittleness number (β_B) and critical value of stress intensity factor (K_C) are also used in present study for the comparison of the results. For

geometrically similar structures, the non-dimensional parameter *brittleness number* of concrete is mathematically expressed as:

$$\beta_B = \frac{D}{l_{ch}} \tag{26}$$

Neglecting the effect of Poisson's ratio as negligible effect in concrete, the critical value of stress intensity factor is evaluated using following relation.

$$K_C = \sqrt{G_{IC} E} \tag{27}$$

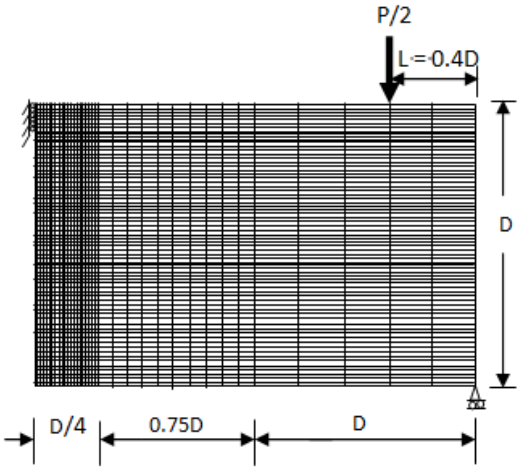

(a) Finite element mesh for half of the FPBT specimen at L = 0.4D

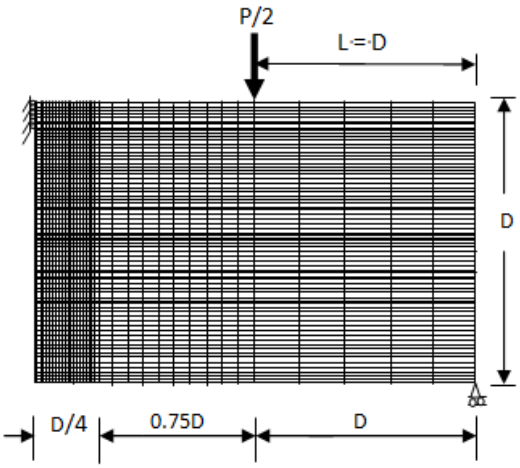

(b) Finite element mesh for half of the FPBT specimen at L = D

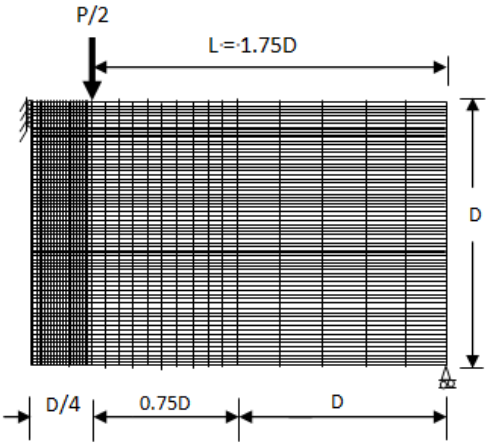

(c) Finite element mesh for half of the FPBT specimen at L = 1.75D

Fig. 5 Finite element discretization of FPBT at different values of shear-span

5. Results and discussion

In the study, pure bending specimens having L = 0.4D, L= D and L = 1.75D and size range 100-500 mm, with varying a_o/D ratios of 0.2, 0.3 and 0.4, are considered. The material constants of concrete are f_t = 3.21MPa, E = 30GPa, G_F = 103 N/m and ν = 0.18 with non-linear softening functions having material constants of c_1=3 and c_2=7 are taken for simulating the FCM. The P-CMOD curves for the various specimens are presented in Figs. 6-9. Peak load and the corresponding $CMOD_c$ obtained from the FCM are used to determine the double-K fracture parameters using inverse analytical method. The same nonlinear softening function is used to determine the double-K fracture parameters. For precise numerical investigation, the effect of self weight of the pure bending beam is considered at all stages of computations. The effect of shear-span/depth ratio on cohesive crack and double-K fracture parameters is presented in the following sections.

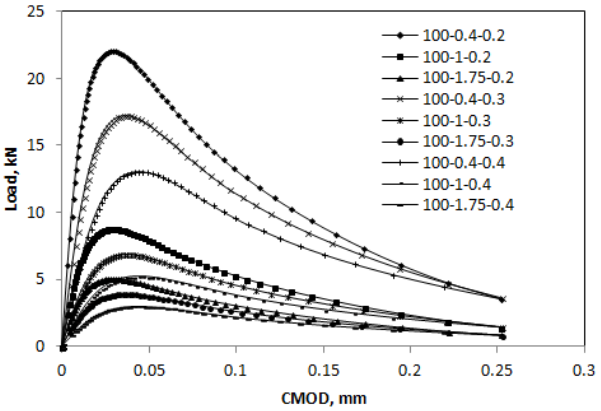

Fig. 6 P-CMOD Curve for specimen size 100mm at different shear-spans/depth ratios and a_0/D ratios

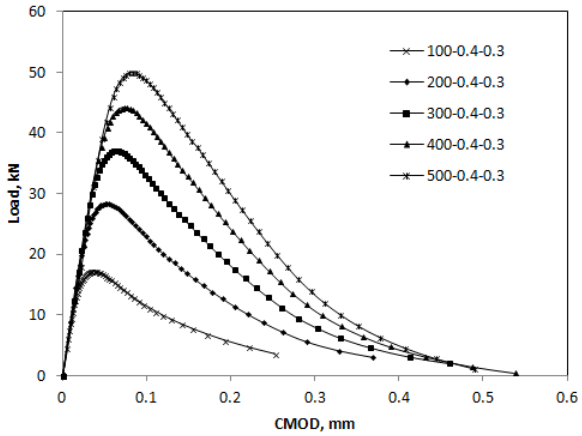

Fig. 7 P-CMOD Curves at shear-spans/depth ratios of 0.4 and different specimen sizes

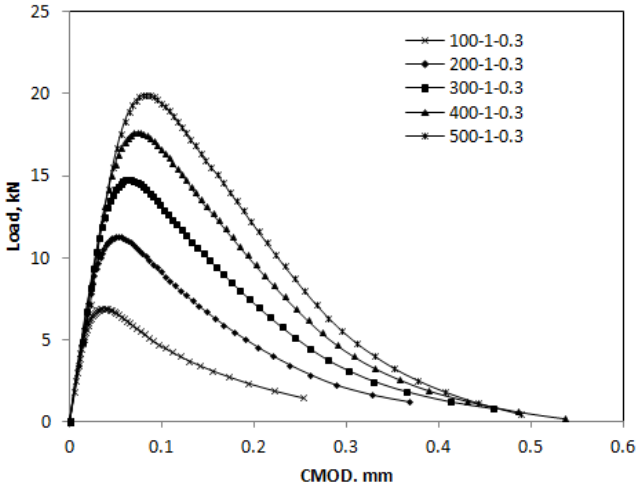

Fig. 8 P-CMOD Curves at shear-spans/depth ratios of 1 and different specimen sizes

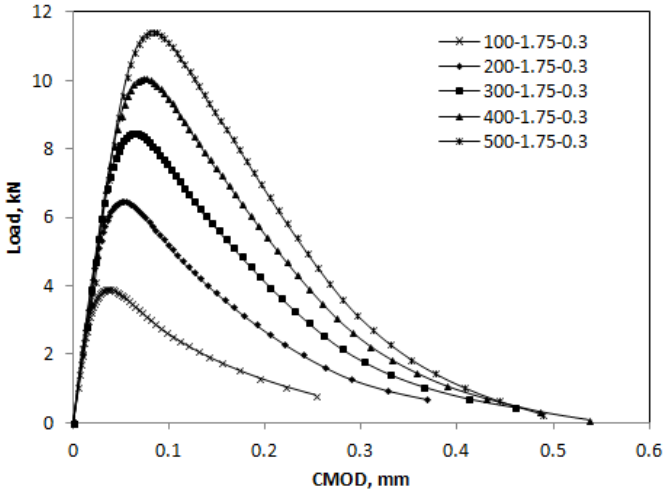

Fig. 9 P-CMOD Curves at shear-spans/depth ratios of 1.75D and different specimen sizes

5.1 Effect of shear –span/depth ratio on cohesive crack fracture parameters

In Figs. 6-9, the legends are presented as specimen size, shear-span/depth ratio and a_o/D ratio. From Fig.6, it is observed that the stiffness and load carrying capacity increases with decrease in the value of a_o/D ratio for a given value of specimen size and shear-span/depth ratio. Also the slope of softening branch increases by decreasing the a_o/D ratio, for a given specimen size and shear-span/depth ratio. As the shear-span/depth ratio increases, the load carrying capacity of the beam specimen decreases at given value of a_o/D ratio and specimen size. The terminal branches of P-CMOD curves appears to be converging and are independent of a_o/D ratio for a given value of

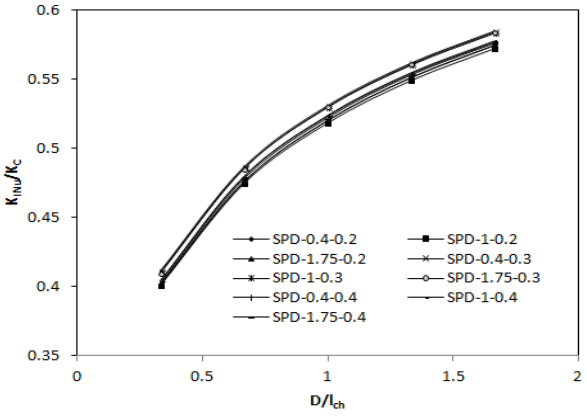

Fig. 10 Size sale transition towards LEFM at different shear-spans/depth ratios and a_0/D ratios

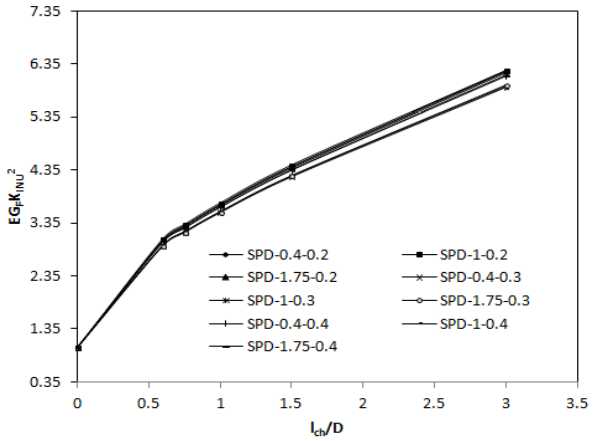

Fig. 11 Size-effect curves for CCM at different shear spans and a_0/D ratios

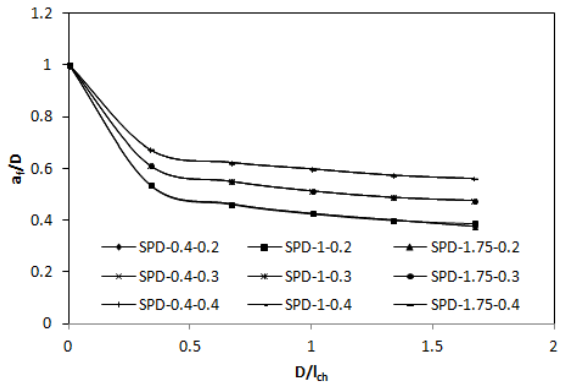

Fig. 12 Variation of fictitious crack length or CCM with the specimen size at different shear-spans/depth ratios and a_0/D ratios

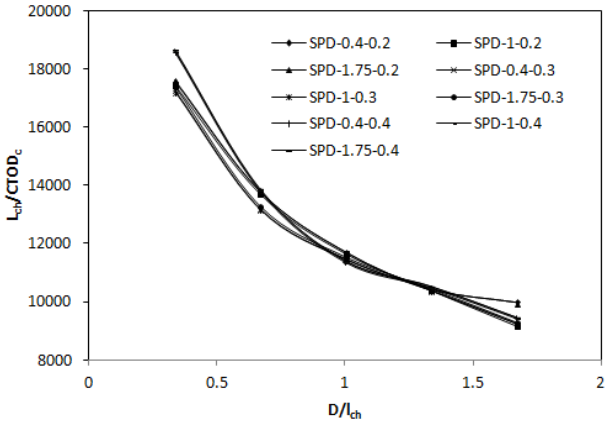

Fig. 13 Relationship between CTODc obtained for CCM and specimen size at different shear-spans/depth ratios and a_0/D ratios

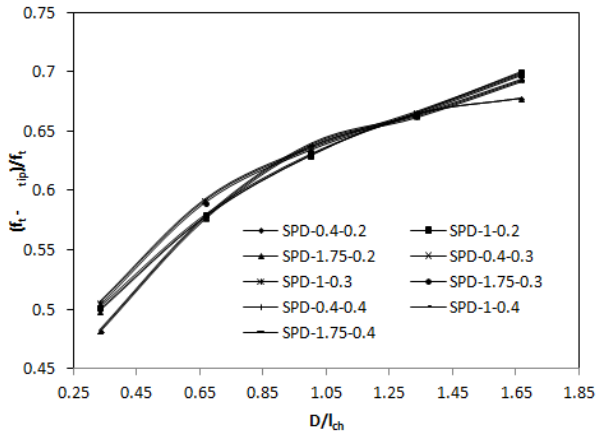

Fig. 14 Relationship between crack tip stress at peak load and specimen size at different shear-spans/depth ratios and a_0/D ratios

shear-span, however these branches follow different paths for different shear-span/depth ratio for a given a_o/D ratio. From Figs.7-9, it can be seen that the load carrying capacity of the specimen, the slope of the softening branch increases with increase in specimen size for a given value of a_o/D ratio and shear –span/depth ratio.

The value of nominal stress intensity factor K_{INu} is determined using the peak load yielded by FCM and the a_o/D ratio. The ratio of K_{INu} / K_c versus *brittleness number* β_B is plotted in Fig.10 to show the deviation from LEFM for geometrical concrete structures at various values of shear-span/depth ratio and a_o/D ratio. The legend in the figure such as SPD-0.4-0.2 represents the shear-span/depth ratio of value 0.4 and a_o/D ratio of 0.2 respectively. It can be observed from the figure that these non-dimensional curves are independent of shear-span/depth ratio and slightly depended on a_o/D ratio for a given specimen size. The cohesive crack size-effect curves obtained at different a_o/D ratios and shear-span/depth ratios are plotted in Fig.11. The figure shows that the size-effect

is also independent of shear span/depth ratio and slightly depended on the a_o/D ratio.

Fictitious crack length/depth (a_f/D) ratio at peak load obtained from FCM at different a_o/D ratio and shear span/depth ratio is plotted versus D/l_{ch} as shown in Fig.12. This relationship indicates that the fictitious crack length at peak load is covered in almost whole ligament for low brittleness of concrete. It is interesting to observe from the figure that a_f/D ratio is independent of shear span/depth ratio for a given value of a_o/D ratio, whereas it depends on a_o/D ratio for a given value of shear-span/depth ratio. The values of a_f/D ratio is obtained as 0.538, 0.613 and 0.675 for a_o/D ratio of 0.2, 0.3 and 0.4 respectively for specimen size of 100mm and these values are 0.375, 0.475 and 0.563 for a_o/D ratio of 0.2, 0.3 and 0.4 respectively for specimen size of 500mm. The values of $CTOD_c$ at peak load are obtained from the simulation of cohesive crack model and these values versus specimen size are plotted in Fig.13. Also the notch-tip stresses σ_{tip} at peak load are obtained from fictitious crack model and the non-dimensional parameter $(f_t-\sigma_{tip})/ f_t$ versus D/l_{ch} are plotted in Fig.14. From Figs.13 and 14 it can be observed that the non-dimensional values of $l_{ch}/ CTOD_c$ and $(f_t-\sigma_{tip})/ f_t$ are almost independent of shear span/depth ratio for a given value of a_o/D ratio whereas these values slightly depend on the a_o/D ratio at constant shear-span/depth.

5.2 Effect of shear-span/depth ratio on double-K fracture parameters

Double-K fracture parameters such as K_{IC}^{un}, K_{IC}^{C} and K_{IC}^{ini} as obtained are plotted with respect to specimen size in non-dimensional form in Figs. 15, 16 and 17 respectively. From Fig.15 it can be seen that the value of K_{IC}^{un} increases with increase in the specimen size and almost independent of shear span/depth ratios. However, it slightly depends on a_o/D ratio.

From Fig.16 it can be observed that the value of K_{IC}^{C} increases with increase in specimen size. It also slightly depends on a_o/D ratio and the variation in the value of K_{IC}^{C} is up to 7% for a_o/D ratio range 0.2 to 0.4. However, the influence of shear-span/depth ratio on K_{IC}^{C} is not appreciable and the variation of K_{IC}^{C} is up to 1% for the shear-span/depth ratio ranging from 0.4 to 1.75. The values of initial cracking toughness for all the specimen can be seen in Fig. 17. It can be seen from the figure that the value of K_{IC}^{ini} decreases with increase in specimen size. The value of K_{IC}^{ini}

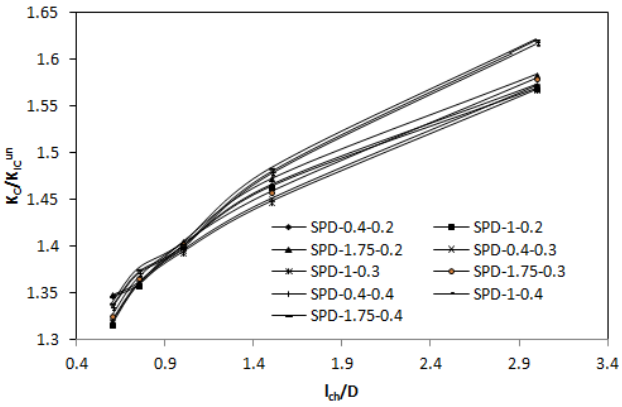

Fig. 15 Relationship between unstable fracture toughness and specimen size at different shear-spans/depth ratios and a_0/D ratios

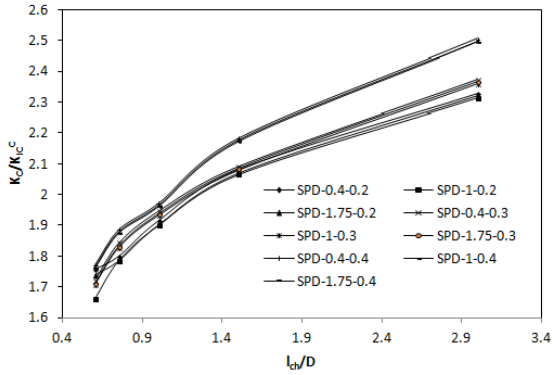

Fig. 16 Relationship between cohesive toughness and specimen size at different shear-spans/depth ratios and a_0/D ratios

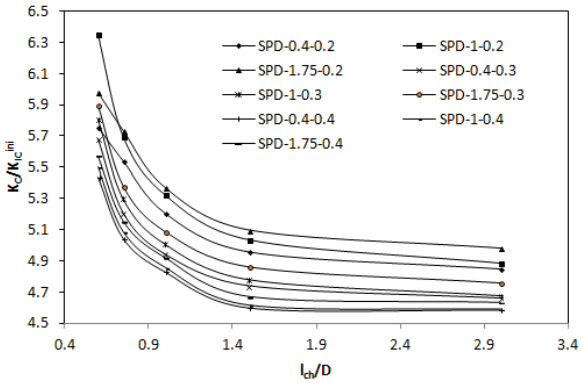

Fig. 17 Relationship between initial cracking toughness and specimen size at different shear-spans/depth ratios and a_0/D ratios

depends on the a_o/D ratio as well as the shear-span/depth ratio. For a given specimen size and shear-span/depth ratio value, the variation in the value of K_{IC}^{ini} is up to 7% for a_o/D ratio ranging from 0.2 to 0.4, whereas, the value of K_{IC}^{ini} varies up to 10% for the shear-span/depth ratio ranging for 0.4 to 1.75 for given specimen size and the a_o/D ratio.

6. Concluding remarks

In present investigation, influence of a shear-span/depth ratio ranging from 0.4 to 1.75 on cohesive crack fracture parameters and double-K fracture parameters of concrete using four point bend test of laboratory size specimen ranging 100-500mm is studied. From the study the following concluding remarks can be mentioned.

• The cohesive crack fracture parameters such as size-effect curves, fictitious crack length at peak load, critical crack tip opening displacement at peak load and crack-tip cohesive stress at peak load are independent of shear-span/depth ratio.

• In double-*K* fracture model, the value of unstable fracture toughness is independent of shear-span/depth ratio whereas, the value of cohesive toughness of the material is slightly dependent on the shear-span/depth ratio. Moreover, the initial cracking toughness is appreciably influenced by shear-span/depth ratio and the variation in initial cracking toughness goes up to 10% when shear-span/depth ratio is varied from 0.4 to 1.75.

Acknowledgements

The authors are grateful to the authority of UGC, New Delhi, India for extending their financial support for carrying out the present work vide sanction letter No. F.No.42-162/2013 (SR). dated 25th March 2013.

References

Barenblatt, G.I. (1962), "The mathematical theory of equilibrium cracks in brittle fracture", *Adv. Appl. Mech*., **7**(1), 55-129.

Bažant ZP (2002), "Concrete fracture models: testing and practice", *Eng. Frac. Mech*., **69**, 165-205.

Bažant, Z.P. and Oh, B.H. (1983), "Crack band theory for fracture of concrete", *Mater. Struct*., **16**(93), 155-177.

Bažant, Z.P., Kim, J.K. and Pfeiffer, P.A. (1986), "Determination of fracture properties from size effect tests", *J. Struct. Eng. ASCE*, **112**(2), 289-307.

Carpinteri, A. (1989), "Cusp catastrophe interpretation of fracture instability", *J. Mech. Phy. Solids*, **37**(5), 567-582.

Carpinteri, A., Cornetti, P., Barpi, F. and Valente, S. (2003), "Cohesive crack model description of ductile to brittle size-scale transition: dimensional analysis vs. renormalization group theory", *Eng. Fract. Mech*., **70**, 1809-1839.

Carpinteri, A., Cornetti P. and Puzzi, S. (2006), "Scaling laws and multiscale approach in the mechanics of heterogeneous and disordered materials", *Appl. Mech. Rev. ASME*, **59**, 283-305.

Cusatis, G. and Schauffert, E.A. (2009), "Cohesive crack analysis of size effect", *Eng. Fract. Mech*., **76**, 2163-2173.

De Borst, R. (2003), "Numerical aspects of cohesive-zone models", *Eng Fract. Mech*., **70**, 1743-1757.

Dugdale, D. S. (1960), "Yielding of steel sheets containing slits", *J. Mech. Phy. Solids*, **8** (2), 100-104.

Elices M., Guinea, G.V., Gómez, J. and Planas, J. (2002), "The cohesive cone model: advantages", limitations and challenges, *Eng. Fract. Mech*., **69**, 137-163.

Elices, M. and Planas, J. (1996), "Fracture mechanics parameters of concrete an overview", *Adv Cem Based Mater*., **4**, 116-127.

Elices, M., Rocco, C. and Roselló, C. (2009), "Cohesive crack modeling of a simple concrete: Experimental and numerical results", *Eng. Fract. Mech*., **76**, 1398-1410.

Glinka, G. and Shen, G. (1991), "Universal features of weight functions for cracks in Mode I", *Eng. Fract. Mech*., **40,** 1135-1146.

Guinea, G.V. (1995), "Modelling the fracture of concrete: the cohesive crack", *Mater. Struct*., **28**(4), 187-194.

Hillerborg, A., Modeer, M. and Petersson, P.E. (1976), "Analysis of crack formation and crack growth in concrete by means of fracture mechanics and finite elements", *Cement Concrete Res*., **6**,773-782.

Hu, S. and Lu, J. (2012), "Experimental research and analysis on Double-K fracture parameters of concrete",

Adv. Sci. Lett., **12** (1), 192-195.
Hu, S., Mi, Z. and Lu, J. (2012), Effect of crack-depth ratio on double-*K* fracture parameters of reinforced concrete", *Appl. Mech. Mater.*, **226-228**, 937-941.
Jenq, Y.S. and Shah, S.P. (1985a), "Two parameter fracture model for concrete", *J. Eng. Mech. ASCE*, **111** (10), 1227-1241.
Jenq, Y.S. and Shah, S.P. (1985b), "A fracture toughness criterion for concrete", *Eng. Fract. Mech.*, **21**, 1055-1069.
Kaplan, M.F. (1961), "Crack propagation and the fracture of concrete", *J. Am. Concrete Inst.*, **58**(5), 591-610.
Karihaloo, B.L. and Nallathambi, P. (1991), *Notched Beam Test: Mode I Fracture Toughness, Fracture Mechanics Test methods for concrete*, *Report of RILEM Technical Committee 89-FMT* (Edited by S.P. Shah and A. Carpinteri), Chamman & Hall, London, 1-86.
Kim, J.K., Lee, Y. and Yi, S.T. (2004), "Fracture characteristics of concrete at early ages", *Cement Concrete Res.*, **34**, 507-519.
Kumar, S. and Barai, S.V. (2008a), "Influence of specimen geometry on determination of double-*K* fracture parameters of concrete: A comparative study", *Int. J. Fract.*, **149**, 47-66.
Kumar, S. and Barai, S.V. (2008b), "Cohesive crack model for the study of nonlinear fracture behaviour of concrete", *J. Inst. Engng. (India)*, CV **89** (Nov.), 7-15.
Kumar, S. and Barai, S.V. (2009a), "Determining double-*K* fracture parameters of concrete for compact tension and wedge splitting tests using weight function", *Eng. Fract. Mech.*, **76**, 935-948.
Kumar, S. and Barai, S.V. (2009b), "Influence of loading condition and size-effect on the K_R-curve based on the cohesive stress in concrete", *Int. J. Fract.*, **156**, 103-110.
Kumar, S. and Barai, S.V. (2009c), "Effect of softening function on the cohesive crack fracture parameters of concrete CT specimen", *Sadhana-Acad. Proc. Eng. Sci.*, **36**(6), 987-1015.
Kumar, S. and Barai, S.V. (2010a), "Determining the Double-*K* fracture parameters for three-point bending notched concrete beams using weight function", *Fatigue Fract. Eng. Mater. Struct.*, **33**(10), 645-660.
Kumar, S. and Barai, S.V. (2010b), "Size-effect prediction from the double-*K* fracture model for notched concrete beam", *Int. J. Damage Mech.*, **19**, 473-497.
Kumar, S. and Barai, S.V. (2012), "Effect of loading condition, specimen geometry, size-effect and softening function on double-*K* fracture parameters of concrete", *Sadhana-Academy Proceedings in Engineering Science*, **37** (Part 1), 3–15.
Kumar, S. and Pandey, S.R. (2012), "Determination of double-*K* fracture parameters of concrete using split-tension cube test", *Comput. Concr. An Int. J.*, **9**(1), 1-19.
Kumar, S., Pandey, S.R. and Srivastava, A.K.L. (2013), "Analytical methods for determination of double-K fracture parameters of concrete", *Adv. Concrete Constr.*, **1(**4), 319-340.
Kwon, S.H., Zhao, Z. and Shah, S.P. (2008), "Effect of specimen size on fracture energy and softening curve of concrete: Part II. Inverse analysis and softening curve", *Cement Concrete Res.*, **38**, 1061-1069.
Murakami, Y. (1987), "Stress Intensity Factors Hand Book", (Committee on Fracture Mechanics, The Society of Materials Science, Japan) Vol-1, Pergamon Press, Oxford.
Murthy, A.R., Iyer N.R. and Prasad, B.K.R (2012), "Evaluation of fracture parameters by Double-G, Double-K models and crack extension resistance for high strength and ultra high strength concrete beams", *Comput. Mater.Continua*, **31**(3), 229-252.
Nallathambi, P. and Karihaloo, B.L. (1986), "Determination of specimen-size independent fracture toughness of plain concrete", *Mag. Concrete Res.*, **38**(135), 67-76.
Park, K., Paulino, G.H. and Roesler, J.R. (2008), "Determination of the kink point in the bilinear softening model for concrete", *Eng. Fract. Mech.*, **7**, 3806-3818.
Petersson, P.E. (1981), "Crack growth and development of fracture zone in plain concrete and similar materials", *Report No. TVBM-100*, Lund Institute of Technology.
Planas, J., Elices, M., Guinea, G.V., Gómez, F.J. Cendón, D.A. and Arbilla, I. (2003), Generalizations and specializations of cohesive crack models, *Eng. Fract. Mech.*, **70**, 1759-1776.
Planas, J. and Elices, M. (1991), "Nonlinear fracture of cohesive material", *Int. J. Fract.*, **51**, 139-157.

Raghu Prasad, B.K. and Renuka Devi, M.V. (2007), "Extension of FCM to plain concrete beams with vertical tortuous cracks", *Eng. Fract. Mech.*, **74**, 2758-2769.
Reinhardt, H.W., Cornelissen, H.A.W. and Hordijk, D.A. (1986), "Tensile tests and failure analysis of concrete", *J. Struct. Eng., ASCE*, **112**(11), 2462-2477.
RILEM Draft recommendation (50-FMC) (1985), "Determination of the fracture energy of mortar and concrete by means of three-point bend test on notched beams", *Mater. Struct.*, **18**, 285-290.
RILEM Draft Recommendations (TC89-FMT) (1990), "Determination of fracture parameters (K_{Ic}^{s} and $CTOD_c$) of plain concrete using three-point bend tests", *Mater. Struct.*, **23**(138), 457-460.
Roesler J., Paulino, G.H., Park, K. and Gaedicke, C. (2007), "Concrete fracture prediction using bilinear softening", *Cement Concrete Compos.*, **29**, 300-312.
Tada, H., Paris, P.C. and Irwin, G. (2000), *The Stress Analysis of Cracks Handbook*, Paris Productions Incorporated, St. Louis, Missouri, USA.
Xu, S. and Reinhardt, H.W. (1998), "Crack extension resistance and fracture properties of quasi-brittle materials like concrete based on the complete process of fracture", *Int. J. Fract.*, **92**, 71-99.
Xu, S. and Reinhardt, H.W. (1999a), "Determination of double-*K* criterion for crack propagation in quasi-brittle materials, Part I: Experimental investigation of crack propagation", *Int. J. Fract.*, **98**, 111-149.
Xu, S. and Reinhardt, H.W. (1999b), "Determination of double-*K* criterion for crack propagation in quasi-brittle materials, Part II: analytical evaluating and practical measuring methods for three-point bending notched beams", *Int. J. Fract.*, **98**, 151-77.
Xu, S. and Reinhardt, H.W. (1999c), "Determination of double-*K* criterion for crack propagation in quasi-brittle materials, Part III: compact tension specimens and wedge splitting specimens", *Int. J. Fract.*, **98**, 179-193.
Xu, S. and Reinhardt, H.W. (2000), "A simplified method for determining double-K fracture meter parameters for three-point bending tests", *Int. J. Fract.*, **104**, 181-209.
Xu, S. and Zhang, X. (2008), "Determination of fracture parameters for crack propagation in concrete using an energy approach", *Eng. Fract. Mech.*, **75**, 4292-4308.
Xu, S. and Zhu, Y. (2009), "Experimental determination of fracture parameters for crack propagation in hardening cement paste and mortar", *Int. J. Fract.*, **157**, 33-43.
Yu, K. and Lu, Z. (2013), "Determining residual double-K fracture toughness of post fire concrete using analytical and weight function method", *Mater. Struct.*, DOI 10.1617/s11527-013-0097-2.
Zhang, X. and Xu, S. (2011), "A comparative study on five approaches to evaluate double-K fracture toughness parameters of concrete and size effect analysis", *Eng. Fract. Mech.*, **78**, 2115-2138.
Zhang, X., Xu, S. and Zheng, S. (2007), "Experimental measurement of double-*K* fracture parameters of concrete with small-size aggregates", *Front. Archit. Civ. Eng. China*, **1**(4), 448-457.
Zhao, Y. and Xu, S. (2002), "The influence of span/depth ratio on the double-*K* fracture parameters of concrete", *J China Three Georges Univ. (Nat. Sci.)*, **24**(1), 35-41.
Zhao, Z., Kwon, S.H. and Shah, S.P. (2008), "Effect of specimen size on fracture energy and softening curve of concrete: Part I. Experiments and fracture energy", *Cement Concrete Res.*, **38**, 1049-1060.
Zi. G. and Bažant, Z.P. (2003), "Eignvalue method for computing size effect of cohesive cracks with residual stress, with application to kink-bands in composites", *Int. J. Eng. Sci.*, **41**, 1519-1534.

CC